AIAA 79-1078R

Approximate Convective-Heating Equations for Hypersonic Flows

E.V. Zoby,* J.N. Moss,† and K. Sutton†
NASA Langley Research Center, Hampton, Va.

Laminar and turbulent heating-rate equations appropriate for engineering predictions of the convective-heating rates about blunt re-entry spacecraft at hypersonic conditions are developed. The approximate methods are applicable to both nonreacting and reacting gas mixtures for either constant- or variable-entropy edge conditions. A procedure which accounts for variable-entropy effects and is not based on mass balancing is presented. Results of the approximate heating methods are in good agreement with available experimental results as well as boundary-layer and viscous-shock-layer solutions.

Nomenclature

c_1, c_2, c_3, c_4, c_5	= defined by Eqs. (9-13)
C_f	= skin-friction coefficient
H	= enthalpy
H_c	= form factor
h	= heat-transfer coefficient
K	= defined by Eq. (2)
M	= Mach number
m	= exponent in friction law
$\dot{m}$	= mass loss rate
N	= reciprocal exponent in velocity profile power law
p	= pressure
Pr	= Prandtl number
$\dot{q}$	= heat-transfer rate
R_N	= nose radius
R_θ	= momentum thickness Reynolds number
$R_{\infty,d}$	= freestream Reynolds number based on base diameter
r	= radius of body of revolution
S	= body wetted length
St	= Stanton number
T	= temperature
u	= velocity
Y	= distance normal to wall
δ	= boundary-layer thickness
δ^*	= displacement thickness
μ	= viscosity
ρ	= density
θ	= momentum thickness
θ_c	= half-cone angle

Subscripts and Superscripts

aw	= adiabatic wall
c	= convective-heating rate
e	= edge conditions
∞	= freestream conditions
L	= laminar
r	= radiative-heating rate
$*$	= conditions determined by reference enthalpy
s	= stagnation-point condition
T	= turbulent
w	= wall condition

Presented as Paper 79-1078 at the AIAA 14th Thermophysics Conference, Orlando, Fla., June 4-6, 1979; submitted Dec. 3, 1979; revision received June 3, 1980. This paper is declared a work of the U.S. Government and therefore is in the public domain.

*Aero-Space Technologist, Aerothermodynamics Branch, Space Systems Division.

†Aero-Space Technologist, Aerothermodynamics Branch, Space Systems Division. Member AIAA.

Introduction

A PROBLEM in the design of most re-entry spacecraft is the prediction of the convective heating-rate distributions. Frequently approximate methods, which have been substantiated by experimental data and/or "benchmark" calculations, are employed in parametric or design calculations. However, current interest in outer-planet entry and advanced-transportation systems for Earth entry has resulted in additional problems for convective-heating analyses. Such problems as arbitrary reactive gas compositions, complex three-dimensional and/or variable-entropy flows, and large surface areas with the possibility of turbulent flow over most of the region are now encountered. Thus, the spacecraft designer needs rapid, but reliable, methods for assessing the effects of such problems on the convective-heating rates.

Although many analytical[1-14] and detailed boundary-layer methods[15-18] are available for convective-heating predictions, many of these methods are restricted to a particular gas composition, stagnation-point solutions, or a perfect-gas analysis. Viscous-shock-layer (VSL) solutions,[19,20] provide a direct means of computing heat fluxes as well as interactions between inviscid and viscous flow regions due to heat transfer, entropy-layer swallowing, and mass injection. However, these methods require large computer run times and storage and are not generally applicable to parametric studies or detailed design calculations.

The purpose of this paper is to investigate existing convective-heating techniques and propose laminar and turbulent heating methods applicable to engineering calculations of nonreacting or reacting flows about blunt re-entry spacecraft. A procedure which accounts for the variable-entropy effects on convective-heating distributions and is not dependent on mass balancing is presented. Results of the approximate methods are compared to experimental results and to boundary-layer and VSL solutions.

Analysis

An approximate convective-heating method has been developed for engineering calculations of laminar and turbulent heating rates about blunt re-entry spacecraft. The approximate method is applicable to nonreacting or reacting gas mixtures for either constant- or variable-entropy edge conditions. This section briefly reviews several approximate laminar and turbulent heating-rate methods and discusses the factors considered in selecting or developing the present methods. Also, this section presents the equations used to calculate the heating rates along with the equations for locating the boundary-layer edge for laminar and turbulent flows influenced by variable entropy.

Existing Heat-Transfer Methods

For both the stagnation-point heating and laminar heating-rate distribution, results based on several analyses[1-4] are in good agreement, but the analyses are restricted to air. For gas compositions other than air, approximate methods are also available.[5,6] The analysis of Sutton and Graves,[5] while limited to the stagnation point of a blunt body, provides a versatile technique of calculating the stagnation-point heat transfer in a wide range of base gases and in mixtures of these gases. The analysis of Marvin and Deiwert[6] provides a method calculating the laminar-heating distribution, but for only a limited number of gas mixtures.

Approximate turbulent heat-transfer expressions[7-14] are primarily based on equating the skin friction to the Stanton number through Reynolds analogy. In Refs. 8-13, the skin-friction relation as a function of the momentum thickness Reynolds number (R_θ) is determined by assuming a velocity profile $[u/u_e=(Y/\delta)^{1/N}]$ to compute the required constants and exponents. For these references, a 1/7th power-law velocity profile is assumed, and differences in the skin-friction equations are due to either the form of the compressible transformations or the value of the form factor ($H_c=\delta^*/\theta$). In Ref. 14, the Spalding-Chi[21] skin-friction relation is used. The Spalding-Chi method has been shown[22] to yield good comparison with experimental ground-test data for heat transfer and skin friction over a wide range of test conditions. However, the method has been shown not to produce the best comparison with flight data.[7]

Present Heat-Transfer Methods

For the stagnation-point heat-transfer calculations, the method of Cohen[2] is used for air calculations, and the method of Sutton and Graves[5] is used for planetary gas mixtures. The equation of Cohen[2] is given as

$$\dot{q}_{w,s}=0.767\ (Pr_w)^{-0.6}(H_s-H_w)(\rho\mu)^{0.43}_{e,s}(\rho\mu)^{0.07}_{w,s}\left(\frac{du}{dS}\right)^{1/2}_{e,s} \tag{1}$$

and the equation of Sutton and Graves[5] is given as

$$\dot{q}_{w,s}=K(p_s/R_N)^{1/2}(H_s-H_w) \tag{2}$$

where K can be determined by a simple but accurate technique[5] over a wide range of gas mixtures. Note that the latter method[5] is also applicable to air calculations and is in good agreement with existing stagnation-point heat-transfer methods.[1-4] The Cohen[2] method is also selected for this investigation due to its wide recognition.

For the calculation of the laminar heat-transfer distribution, a method similar to that presented in Refs. 2-4 and 6 is not available for application to a wide range of gas mixtures. Thus, the laminar distributions are computed herein by relating heat transfer to a skin-friction relation based on R_θ through a modified Reynolds analogy form. This approach is useful since a momentum or boundary-layer thickness will be required for approximating the variable-entropy effects on the heat-transfer calculations. The laminar heat transfer is computed using the incompressible Blasius[23] relation, with compressibility effects accounted for by Eckert's reference enthalpy relation,[24] and is given by

$$\dot{q}_{w,L}=0.22(R_{\theta,e})^{-1}(\rho^*/\rho)(\mu^*/\mu)\rho_e u_e \times (H_{aw}-H_w)(Pr_w)^{-0.6} \tag{3}$$

where θ is computed by

$$\theta_L=0.664\left(\int_0^S\rho^*\mu^*u_e r^2 dS\right)^{1/2}\Big/(\rho_e u_e r) \tag{4}$$

Equation (4) provides a technique to include the effect of geometry and variable-edge conditions about a blunt body on the laminar momentum-thickness calculation. The equation reduces to the standard Blasius form for flat-plate assumptions.

The turbulent heat transfer is also computed by using a skin-friction coefficient based on R_θ. Published results[8-13] using this form for the skin-friction relation assume a 1/7th velocity profile and use values of H_c varying from -1.0 to 9/7. It is noted[25] that the 1/7th profile is not applicable over an extensive Reynolds number range. Libby and Cresci[8] illustrate the insensitivity of the turbulent heat transfer to the form factor for values of approximately 1.0 or less. In Ref. 11, the authors present several reasons for using $H_c=-1$ in hypersonic turbulent boundary-layer calculations. Also, since this value of H_c was used by Lees[26] in developing a hypersonic laminar method, a value of $H_c=-1.0$ is used in this analysis. Although the turbulent-heating analyses[8-13] adopt a constant value of N equal to 7, experimental results[27] show N to be a function of R_θ with values of N as low as 4 for R_θ equal to approximately 1000. A compressible turbulent analysis[28] has demonstrated the effect of a variable N on the skin friction. In order to incorporate this effect in the present analysis, the skin friction is assumed as

$$c_f/2=c_1(R_{\theta,e})^{-m} \tag{5}$$

which, after substituting in the momentum equation and integrating, yields an expression for the turbulent momentum growth as

$$\theta_T=\left(c_2\int_0^S\rho^*u_e\mu^{*m}r^{c_3}dS\right)^{c_4}\Big/(\rho_e u_e r) \tag{6}$$

where m, c_1, c_2, c_3, and c_4 are functions of N.[25,28] This integral expression for the turbulent momentum thickness is similar in nature to Eq. (4) for the laminar momentum thickness. A curve fit of axisymmetric nozzle-wall data[27] produces

$$N=12.67-6.5\log(R_{\theta e})+1.21(\log R_{\theta,e})^2 \tag{7}$$

The N values presented[27] for axisymmetric nozzle-wall tests at R_θ less than approximately 10^4 are generally lower than corresponding N values based on sharp-cone or flat-plate conditions. Thus, for R_θ values less than 10^4, the present skin-friction results would not be in good agreement with standard flat-plate incompressible methods.

Relations for the coefficients and exponents in Eqs. (5) and (6) are given as

$$m=2/(N+1) \tag{8}$$

$$c_1=(1/c_5)^{2N/(N+1)}[N/(N+1)(N+2)]^m \tag{9}$$

$$c_2=(1+m)c_1 \tag{10}$$

$$c_3 = 1 + m \tag{11}$$

$$c_4 = 1/c_3 \tag{12}$$

$$c_5 = 2.2433 + 0.93N \tag{13}$$

With Eq. (5) and a modified Reynolds analogy form, the resulting turbulent heat-transfer equation is

$$\dot{q}_{w,T} = c_1 (R_{\theta,e})^{-m} (\rho^*/\rho_e)(\mu^*/\mu_e)^m \rho_e u_e \times (H_{aw} - H_w)(Pr_w)^{-0.4} \tag{14}$$

The exponents used for the Prandtl number in Eqs. (3) and (14) are based on results presented by Kays.[29] Also, the Prandtl number is evaluated herein as the frozen Prandtl number evaluated at the wall temperature.

Application to Three-Dimensional Flow

Based on the axisymmetric analog,[30,31] simplifying assumptions can be applied to the complex three-dimensional boundary-layer theory which allows equations such as presented herein to be modified for three-dimensional heating-rate calculations. As a result of these assumptions, the distance along a streamline is substituted for the distance S along the body surface, and the metric coefficient for the surface coordinate normal to the streamline is used rather than the cross-sectional radius r. The calculated results of procedures[31,32] using the axisymmetric analog have been shown to be in good agreement with measured three-dimensional heating data.

Local Conditions

Heat-transfer calculations, based on integral or detailed boundary-layer techniques, require inviscid properties external to the boundary layer. Usually, the external flow is assumed to be at a constant-entropy condition corresponding to either the oblique-shock or stagnation-streamline entropy. In general, however, the assumption of a constant-entropy value does not provide an adequate description of the external flow properties over the entire length of a blunt body in high-speed flow. This situation is caused by the highly curved shocks produced by blunt bodies. These shocks generate entropy gradients in the inviscid flow, resulting in inviscid velocity gradients normal to the body surface.[33] Streamlines of varying entropy value, which pass through different points on the shock, are gradually embedded in the boundary layer as the layer grows along the surface. Thus, this process, referred to as streamline swallowing, results in variable-entropy conditions at the boundary-layer edge.

There are at least two techniques which account for the effect of variable-entropy flows on the surface heat transfer and skin friction. One method is the VSL solution[19,20] which provides a direct means of accounting for the entropy-gradient effects since the VSL equations are valid throughout the shock layer. However, these methods do require large computer run times and storage. Another method which is employed in approximate integral or detailed boundary-layer codes is mass balancing. The iterative mass-balancing procedure equates the mass flow in the boundary layer at the body point of interest to a streamtube of equal mass in the freestream.[33] Hence, for mass-balancing procedures, the shock shape and pressure distribution about the blunt body are required. The results of such calculations have been demonstrated for blunt bodies at 0-deg incidence.[13-15,33-36] Note that these results are obtained primarily at high laminar Reynolds number flow conditions and for turbulent flows at stations far downstream on long slender blunt cones, i.e., at such conditions where vorticity interaction is weak. At these conditions, the comparisons of the computational and experimental results are good. However, for regions of strong vorticity interaction, e.g., turbulent flow over outer-planet probes which are relatively short blunt bodies with large half-angle afterbodies, calculated results of turbulent integral and detailed boundary-layer analyses employing mass-balancing techniques are shown to overpredict corresponding VSL heat-transfer results by 30-40%.[37] Anderson and Wilcox[37] attribute the too-rapid "swallowing" of the high-entropy flow to the fact that detailed boundary layer codes do not usually account for the nonvanishing value of $(\partial u/\partial y)_e$ in the boundary conditions. This term tends to suppress the boundary-layer growth. The discrepancies are greater in turbulent-heating comparisons where the boundary-layer and displacement thicknesses determine the scale of turbulence. A boundary-layer analysis[38] which accounts for the $(\partial u/\partial y)_e$ term reports good comparisons (within 10%) with VSL results. For the approximate integral methods, the inclusion of such a term is not feasible. In addition, the typically assumed 1/7th power-law velocity profile may not always be appropriate for the particular local flow conditions.

For blunt bodies at incidence, the required mass-balancing technique presents at best a complex procedure.[39] Currently, there are existing solution procedures for sharp cones at incidence[39] and for the windward ray of blunt axisymmetric bodies.[40]

Considering the inherent difficulties involved with applying mass balancing to three-dimensional flow and the apparent discrepancies resulting from approximate or classical boundary-layer methods for axisymmetric flows, a somewhat different approach for approximating variable entropy is used in this study.

An inviscid solution is assumed to be known. Then, by means of an iterative process, the momentum-thickness Eqs. (4) and (6) and corresponding approximate ratios of boundary-layer thickness to momentum thickness are used to determine the local flow conditions. Thus, this analysis accounts for variable-entropy effects by locally moving out in the inviscid flowfield at a distance equal to the boundary-layer thickness. The inviscid properties at this location are used as the boundary-layer edge properties. This concept was recently suggested by Popinski[18] for three-dimensional flows. Thus, this method of determining variable-entropy edge conditions coupled with the axisymmetric analog appears to offer a simpler method for three-dimensional heat-transfer calculations. In this investigation, the boundary-layer thickness to momentum-thickness ratios[41,42] used are

$$(\delta/\theta)_L = 5.55 \tag{15}$$

and

$$\left(\frac{\theta}{\delta}\right)_T = N + 1 + \left[\left(\frac{N+2}{N}\frac{H_w}{H_{aw}} + 1\right) \times \left(1 + 1.29\left(Pr_w\right)^{0.333}\frac{u_e^2}{2H_e}\right)\right] \tag{16}$$

The results of Eq. (16) when coupled with Eqs. (6) and (14) will be demonstrated herein to provide good agreement with turbulent VSL solutions in regions of strong vorticity interactions.

Results and Discussion

In this section, results obtained with the present approximate laminar and turbulent heating-rate equations are compared with available experimental results as well as with boundary-layer and VSL solutions. Initially, the results of the approximate methods are compared with perfect and reacting gas boundary-layer solutions and existing blunt-body experimental heat-transfer data. Secondly, the results of the approximate methods are compared with perfect and reacting

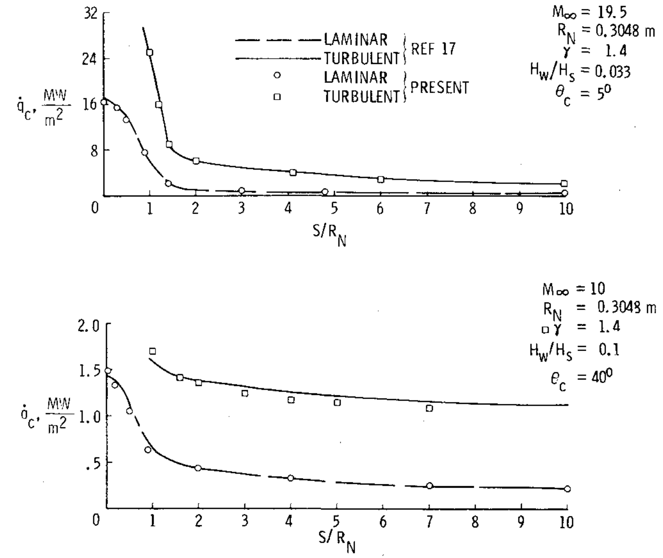

Fig. 1 Comparisons of convective heating-rate distributions at constant-entropy conditions: a) 5-deg sphere cone, b) 40-deg sphere cone.

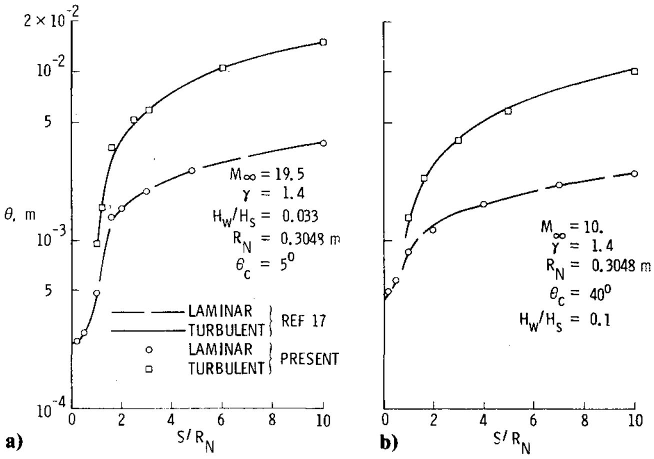

Fig. 2 Comparisons of boundary-layer momentum-thickness distributions at constant-entropy conditions: a) 5-deg sphere cone, b) 40-deg sphere cone.

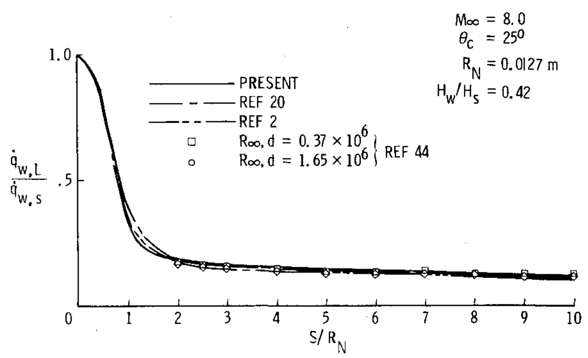

Fig. 3 Comparison of experimental and calculated laminar heating-rate distributions.

gas VSL solutions. All comparisons are for 0-deg angle-of-attack conditions. These comparisons should validate the present approximate methods for engineering applications to either nonreacting or reacting flows at both constant- and variable-entropy edge conditions. For the constant-entropy conditions, the local flow conditions are determined by expanding the flow from the normal-shock stagnation-point condition to the local pressure.

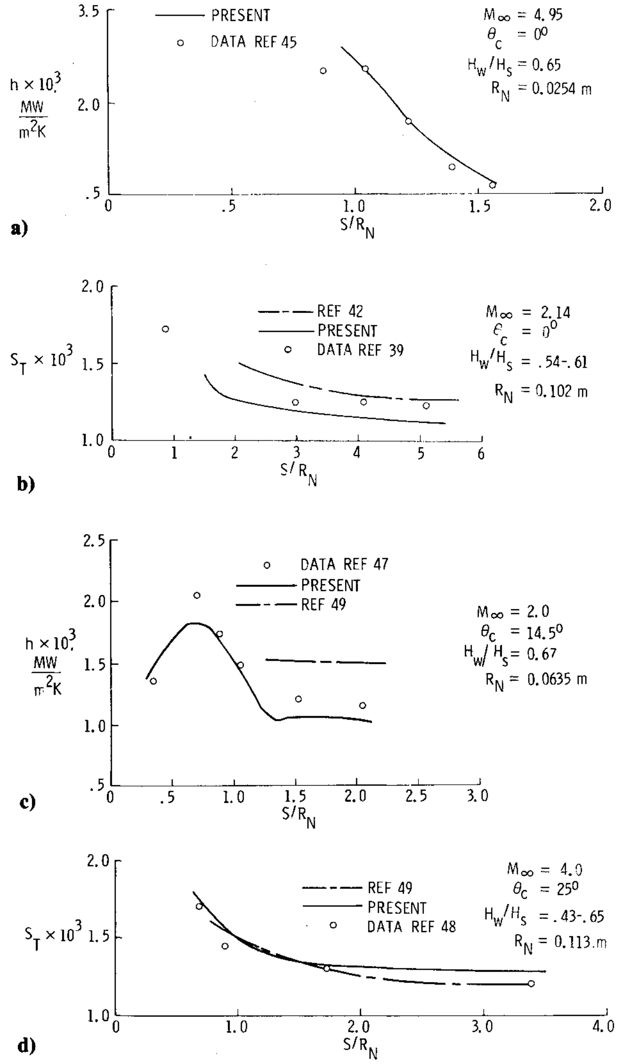

Fig. 4 Comparison of experimental and calculated turbulent heating-rate distributions: a) hemisphere, b) hemisphere-cylinder, c) 14½-deg sphere cone, d) 25-deg sphere cone.

Constant-Entropy Conditions

Perfect-gas boundary-layer solutions[17] of laminar and turbulent heating rates about a blunt 5-deg cone at $M_\infty = 19.5$, $\gamma = 1.4$, and $H_w/H_s = 0.033$ and about a blunt 40-deg cone at $M_\infty = 10.0$, $\gamma = 1.4$, and $H_w/H_s = 0.1$ are presented in Figs. 1a and 1b, respectively. For both conditions, the approximate heat-transfer results predicted by the laminar [Eq. (3)] and the turbulent [Eq. (14)] methods are in good agreement with the corresponding boundary-layer solution with differences of less than 10% noted. Although not shown on the figure, good agreement with existing approximate laminar methods[4,43] are obtained for both conditions. However, results based on existing turbulent methods[8-12] are as much as 20% lower than the boundary-layer results for the blunt 5-deg cone and within +40 and −20% of the boundary-layer results for the blunt 40- deg cone. For the two cases, the corresponding growth of the laminar and turbulent boundary-layer momentum thickness predicted by Eqs. (4) and (6) is shown in Figs. 2. Good comparisons are obtained with the boundary-layer solutions.[17]

Experimental laminar and turbulent heat-transfer data are presented in Figs. 3 and 4. The laminar data[44] are compared with results of Eq. (3), the heating distribution of Cohen,[2] and a VSL solution.[20] Note that no significant entropy-gradient effects on the heat transfer are observed based on the comparison of the constant-entropy and VSL results. The turbulent data[45-48] are compared with the results of Eq. (14)

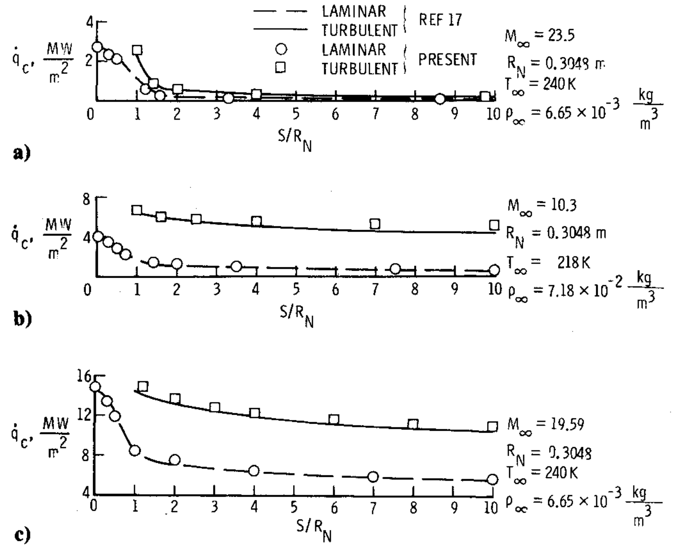

Fig. 5 Comparison of convective-heating data distributions at constant-entropy conditions for equilibrium air: a) 5-deg sphere cone, b) 40-deg sphere cone, c) 40-deg sphere cone.

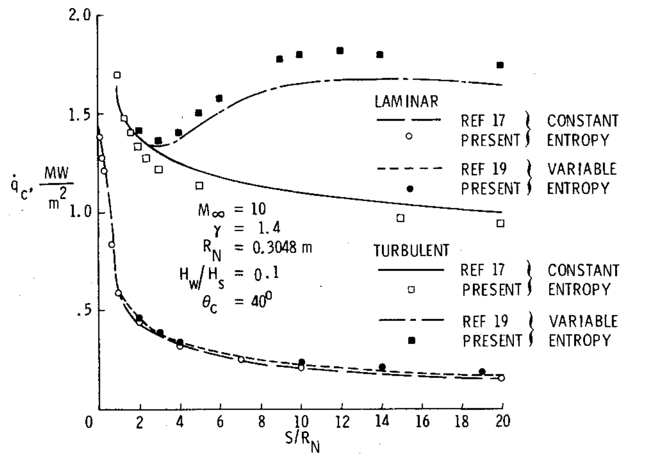

Fig. 6 Comparison of convective heating-rate distributions.

and, when presented in the cited references, the method of Van Driest.[49] The comparison of the laminar and turbulent data with the present approximate results is good (approximately 10%).

Calculated results for equilibrium air are shown for several conditions in Fig. 5. Discrepancies of less than 15% are noted in the comparison of the boundary-layer solutions[17] and the approximate laminar and turbulent results.

Variable-Entropy Conditions

The effect of variable entropy on the heat transfer is illustrated in Figs. 6 and 7. Boundary-layer[17] and VSL[19] solutions of the laminar and turbulent heating distributions about a 40-deg cone at $M_\infty = 10.0$, $\gamma = 1.4$, and $H_w/H_s = 0.1$ are presented in Fig. 6. For these conditions, results of the laminar VSL calculations show only a slight increase (less than 10%) over the boundary-layer results up to 20-nose radii. However, over this same length, a 65% increase is noted in the turbulent VSL results compared to the boundary-layer values. The results of the present approximate laminar and turbulent heat-transfer calculations for both constant- and variable-entropy conditions are also shown in Fig. 6. The impact of entropy swallowing on the heat transfer is approximately accounted for herein by defining the boundary-layer edge properties as the inviscid values located at a distance from the surface equal to the boundary-layer thickness. For the

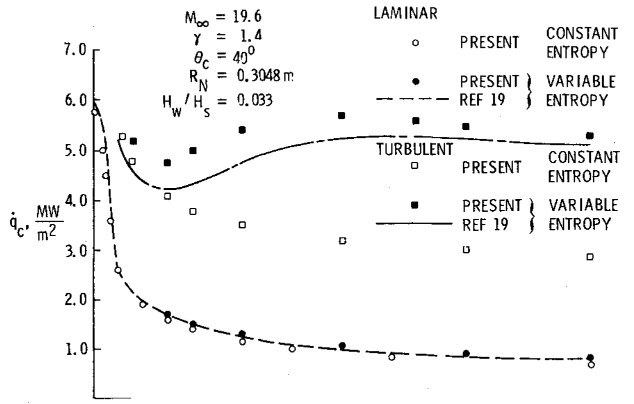

Fig. 7 Comparison of convective heating-rate distributions.

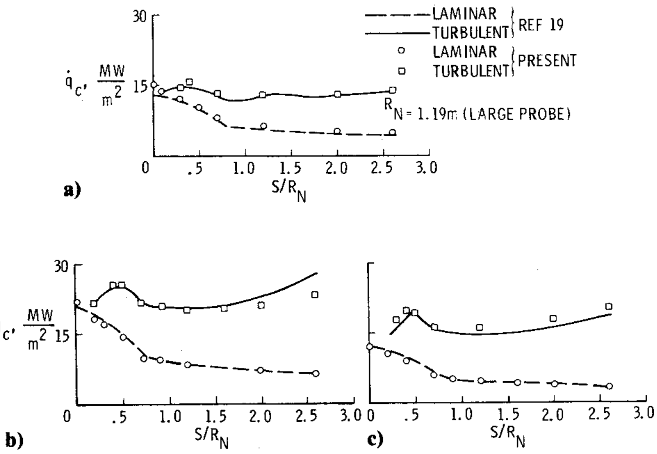

Fig. 8 Comparison of convective heating-rate distributions for Venusian atmosphere: a) $U_\infty = 11.38$ km/s, b) $U_\infty = 10.82$ km/s, c) $U_\infty = 7.54$ km/s.

variable-entropy heating results shown in Fig. 6, an iterative solution is employed using an inviscid flowfield calculation,[50] Eqs. (3), (4), and (15) for the laminar predictions, and Eqs. (6), (14), and (16) for the turbulent results. The approximate variable-entropy heat-transfer predictions are in good agreement with VSL[19] results (less than 15% disagreement). These comparisons are in contrast to the results presented for the same conditions in Ref. 37 where discrepancies of 40% were noted between VSL solutions and boundary-layer methods using mass balancing. Similar comparisons are also obtained for the results presented in Fig. 7 for a 40-deg blunt cone at $M_\infty = 19.6$, $\gamma = 1.4$, and $H_w/H_s = 0.033$ and at these same conditions for a 15-deg hyperboloid (results not presented).

Typical VSL convective-heating distributions about the Venusian entry large probe ($\theta_c = 45$ deg, $R_N = 1.19$ m) at several trajectory points are presented in Fig. 8. The inviscid flowfield technique of Falanga and Olstad[51] is coupled with the approximate variable-entropy heat-transfer calculations. The VSL and approximate laminar heating-rate results are in good agreement (within 10%). Generally, good agreement is also obtained for the turbulent heating-rate comparisons with a maximum discrepancy of approximately 18%.

Comparisons for the nominal Jovian entry conditions are presented in Figs. 9 and 10 with similar agreement. The results presented in Fig. 9 are for an adiabatic flowfield, whereas the results of Fig. 10 are computed for a radiating flowfield. The inviscid flowfield calculation, which is coupled with the approximate method, is based on the procedure of Zoby et al.[52] Note that for the calculation of the outer eddy viscosity in the turbulent VSL solutions,[53] the location of the boun-

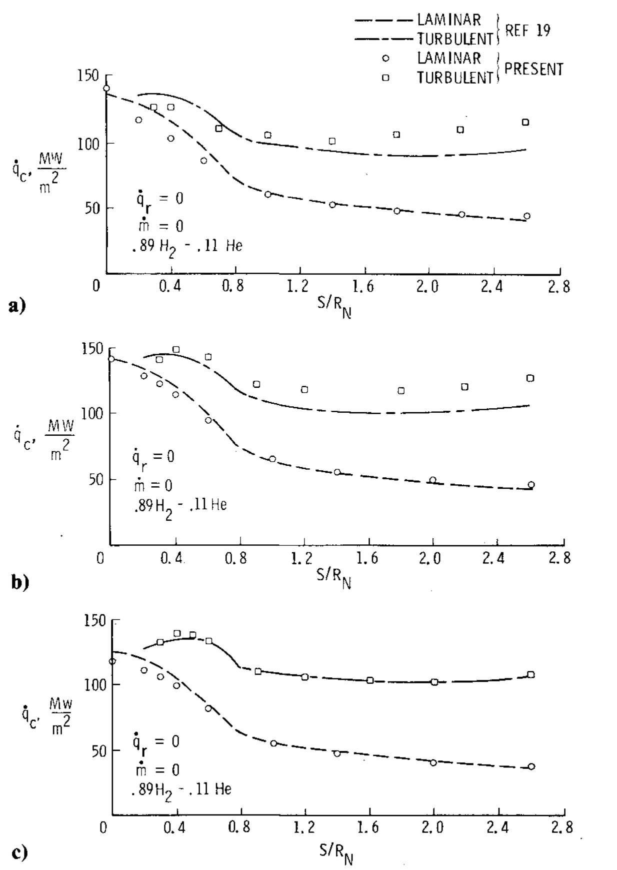

Fig. 9 Comparison of convective heating-rate distributions for Jovian atmosphere: a) $U_\infty = 42.88$ km/s, b) $U_\infty = 39.28$ km/s, c) $U_\infty = 34.67$ km/s.

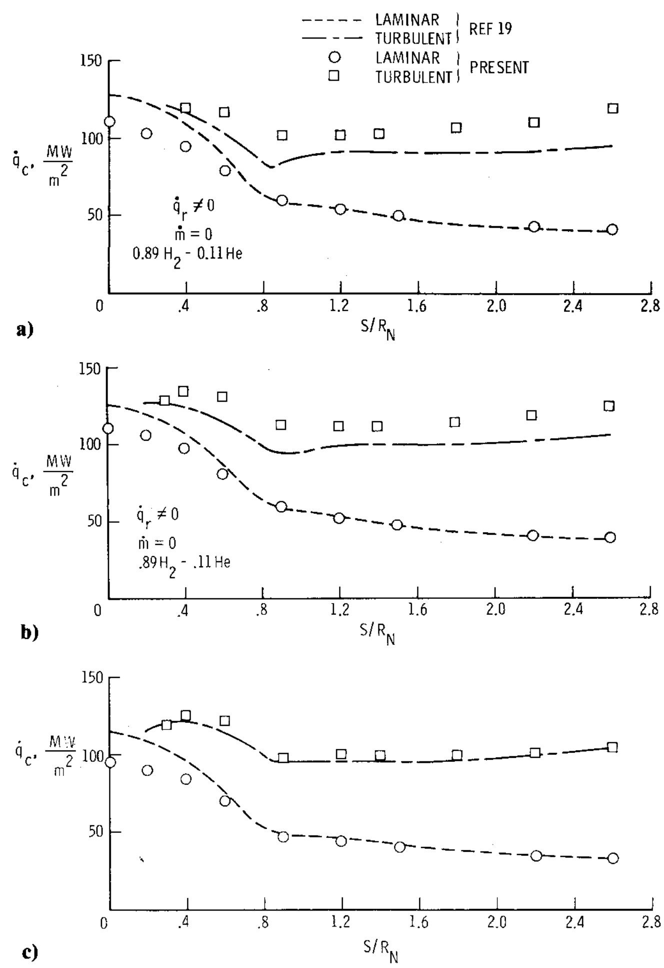

Fig. 10 Comparison of convective heating-rate distributions with radiating flowfield for Jovian conditions: a) $U_\infty = 42.88$ km/s, b) $U_\infty = 39.28$ km/s, c) $U_\infty = 34.67$ km/s.

dary-layer thickness is assumed to be determined at a value of $H/H_s = 0.995$ in nonradiative calculations and at an index of dissipation equal to 0.95 for radiating flowfields. An evaluation of these limits indicated a poor match of the boundary-layer thickness for nonradiative calculations. A value of the dissipation index equal to 0.98 gave a much better comparison with the boundary-layer thickness predicted by the $H/H_s = 0.995$ limit. Thus, the VSL turbulent heating rates presented in Fig. 10 use a dissipation index of 0.98.

Note that while good agreement is obtained with the present laminar variable-entropy method and VSL solutions, comparisons at conditions of low Reynolds number flow or far downstream on a blunt body may better substantiate the validity of Eq. (15). However, the previous comparisons have demonstrated that the present heating-rate methods provide reliable estimations of blunt-body heat-transfer rates over a wide range of gas compositions and in regions of strong vorticity interactions (for turbulent flow).

For parametric or design calculations, the spacecraft designer is concerned with the computer time required as well as with the reliability of the heating method. For the variable-entropy comparisons presented herein, the engineering heating-rate methods have been coupled with rapid, but reliable, inviscid flowfield methods.[50-52] As a point of interest, the present turbulent variable-entropy calculations [(Eqs. (6), (14), and (16) coupled with inviscid-flow calculations[50]] presented in Fig. 6 required approximately 22 s on the CDC 6600 computer, while the VSL solution required 240 s. The boundary-layer mass-balancing procedure, which includes the $(\partial u/\partial y)_e$ term[38] (not presented), required approximately 150 s.

Conclusions

Approximate laminar and turbulent heat-transfer equations are developed for the engineering prediction of convective-heating rates about blunt-entry spacecraft in hypersonic flow. The equations are applicable to nonreacting or reacting gas flows at conditions of constant or variable entropy. The variable-entropy effect on the heat transfer was approximated by defining the boundary-layer edge properties as the inviscid values located a distance from the surface equal to the boundary-layer thickness.

Details of the stagnation point and the local laminar and turbulent heat-transfer equations are given. Also, equations for computing the laminar and turbulent momentum thicknesses and for computing the corresponding ratios of boundary-layer thickness to momentum thickness are presented.

The results of the approximate methods are in good agreement with available experimental heat-transfer data as well as boundary-layer and viscous-shock-layer solutions. The method provides a rapid, but reliable, technique for the prediction of convective-heating rates in parametric or design studies.

References

[1] Fay, J.A. and Riddell, F.R., "Theory of Stagnation-Point Heat Transfer in Dissociated Air," *Journal of Aerospace Sciences*, Vol. 25, No. 2, Feb. 1958, pp. 73-85, 121.

[2] Cohen, N.B., "Boundary-Layer Similar Solutions and Correlation Equations for Laminar Heat-Transfer Distribution in Equilibrium Air at Velocities Up to 41,100 Feet Per Second," NASA TR R-118, 1961.

[3] Kemp, N.H., Rose, P.H., and Detra, R.W., "Laminar Heat Transfer Around Blunt Bodies in Dissociated Air," *Journal of Aerospace Sciences*, Vol. 26, No. 7, July 1959, pp. 421-430.

[4] Zoby, E.V., "Approximate Relations for Laminar Heat Transfer and Shear Stress Functions in Equilibrium Dissociated Air," NASA TN D-4484, April 1968.

[5]Sutton, K. and Graves, R.A., Jr., "A General Stagnation Point Convective Heating Equation for Arbitrary Gas Mixtures," NASA TR R-376, Nov. 1971.

[6]Marvin, J.G. and Deiwert, G.S., "Convective Heat Transfer in Planetary Gases," NASA TR R-224, July 1965.

[7]Zoby, E.V. and Graves, R.A., Jr., "Comparison of Results from Three Prediction Methods With Turbulent-Heating Data from Wind Tunnel and Free-Flight Tests," NASA TM X-2390, Sept. 1971.

[8]Libby, P.A. and Cresci, R.J., "Evaluation of Several Hypersonic Turbulent Heat Transfer Analyses by Comparison With Experimental Data," WADC TN 57-72, July 1957.

[9]Phillips, R.L., "A Summary of Several Techniques Used in the Analysis of High Enthalpy Level, High Cooling Ratio Turbulent Boundary Layers on Blunt Bodies of Revolution," Ramo Wooldridge Corp., GM-TM-194, Sept. 1957.

[10]Vaglio-Laurin, R., "Turbulent Heat Transfer on Blunt Nosed Bodies in Two-Dimensional and General Three-Dimensional Hypersonic Flow," *Journal of Aerospace Sciences*, Vol. 27, No. 1, Jan. 1960, pp. 27-36.

[11]Cresci, R.J., MacKenzie, D.A., and Libby, P.A., "An Investigation of Laminar, Transitional, and Turbulent Heat Transfer on Blunt-Nosed Bodies in Hypersonic Flow," *Journal of Aerospace Sciences*, Vol. 27, No. 6, June 1960, pp. 401-414.

[12]Hartley, D.L. and Witze, P.D., "Turbulent Heating From a Compressible Boundary Layer With Pressure Gradient," Sandia Labs., SCL RR-69-70, Oct. 1969.

[13]Edquist, C.T., "A Technique for Predicting Shock Induced Vorticity Effects During Venus Entry," Martin Marietta Corp., R-70-48671-006, Aug. 1970.

[14]Johnson, C.B. and Boney, L.R., "A Simple Integral Method for the Calculation of Real-Gas Turbulent Boundary Layers With Variable Edge Entropy," NASA TN D-6217, June 1971.

[15]Stainback, P.C. (with Appendix by P.C. Stainback and K.C. Wicker), "Effect of Unit Reynolds Number, Nose Bluntness, Angle of Attack, and Roughness on Transition on a 5° Half-Angle Cone at Mach 8," NASA TN D-4961, 1969.

[16]Harris, J.E., "Numerical Solutions of the Equations for Compressible Laminar, Transitional, and Turbulent Boundary Layers and Comparisons With Experimental Data," NASA TR R-368, Aug. 1971.

[17]Anderson, E.C. and Lewis, C.H., "Laminar or Turbulent Boundary-Layer Flows of Perfect Gases or Reacting Gas Mixtures in Chemical Equilibrium," NASA CR-1893, Oct. 1971.

[18]Popinski, Z., "Compressible Laminar Boundary Layers on Sharp Cones at Incidence With Entropy Swallowing," *AIAA Journal*, Vol. 13, No. 9, Sept. 1975, pp. 1135-1136.

[19]Moss, J.N., "Stagnation and Downstream Viscous Shock Layer Solutions With Radiation and Coupled Ablation Injection," AIAA Paper 74-73, Jan. 1974.

[20]Kumar, A. and Graves, R.A., Jr., "Numerical Solution of the Viscous Hypersonic Flow Past Blunted Cones at Angle of Attack," AIAA Paper 77-172, Jan. 1977.

[21]Spalding, D.B. and Chi, S.W., "The Drag of a Compressible Turbulent Boundary Layer on a Smooth Flat Plate With and Without Heat Transfer," *Journal of Fluid Mechanics*, Vol. 18, Pt. 1, Jan. 1964, pp. 117-143.

[22]Cary, A.M., Jr. and Bertram, M.H., "Engineering Predictions of Turbulent Skin Friction and Heat Transfer in High Speed Flow," NASA TN D-7507, 1974.

[23]Schlichting, H., *Boundary-Layer Theory*, 4th Ed., McGraw-Hill, New York, 1960.

[24]Eckert, E.R.G., "Survey on Heat Transfer at High Speeds," U.S. Air Force, ARL 189, Dec. 1961.

[25]White, F.M., *Viscous Fluid Flow*, McGraw-Hill, New York, 1974.

[26]Lees, L., "Laminar Heat Transfer Over Blunt Bodies at Hypersonic Flight Speeds," *Jet Propulsion*, Vol. 26, No. 4, April 1956, pp. 259-269, 274.

[27]Johnson, C.B. and Bushnell, D.M., "Power-Law Velocity-Profile-Exponent Variations With Reynolds Number, Wall Cooling, and Mach Number in a Turbulent Boundary Layer," NASA TN D-5753, April 1970.

[28]Kutateladze, S.S. and Leont'ev, A.I., *Turbulent Boundary Layers in Compressible Gases*, Academic Press, Inc., New York, 1964.

[29]Kays, W.M., *Convective Heat and Mass Transfer*, McGraw-Hill, New York, 1966.

[30]Cooke, J.C., "An Axially Symmetric Analogue for General Three-Dimensional Boundary Layers," *Ministry of Aviation*, A.R.C. Technical Report, R&M No. 3200, June 1959.

[31]DeJarnette, F.R. and Hamilton, H.H., "Inviscid Surface Streamlines and Heat Transfer on Shuttle-Type Configurations," *Journal of Spacecraft and Rockets*, Vol. 10, No. 6, May 1973, pp. 314-321.

[32]Hamilton, H.H. II, "Calculation of Heating Rates on Three-Dimensional Configurations," Degree of Engineering Thesis, George Washington University, Dec. 1979.

[33]Ferri, A., "Some Heat-Transfer Problems in Hypersonic Flow," *Aeronautics and Astronautics*, Pergamon Press, New York, 1960, pp. 344-377.

[34]Witze, P.O. and Hartley, D.C., "Assessment of the Proper Boundary Conditions at the Outer Edge of the Turbulent Boundary Layer on Spherically Blunted Conical Bodies," Sandia Labs., SCL-RR-69-67, Sept. 1969.

[35]Mayne, A.W., Jr. and Adams, J.C., Jr., "Streamline Swallowing By Laminar Boundary Layers in Hypersonic Flow," AEDC-TR-71-32, March 1971.

[36]Mayne, A.W., Jr., and Dyer, D.F., "Comparisons of Theory and Experiment for Turbulent Boundary Layers on Simple Shapes at Hypersonic Conditions," *Proceedings of the 1970 Heat Transfer and Fluid Mechanics Institute*, Stanford University Press, June 1970, pp. 168-188.

[37]Anderson, E.C. and Wilcox, D.C., "Vorticity Interaction Effects on Blunt Bodies," NASA CR-2778, Jan. 1977.

[38]Anderson, E.C. and Wilcox, D.C., "Transitional Boundary-Layer Solutions Using a Mixing-Length and a Two-Equation Turbulence Model," NASA CR-2986, April 1978.

[39]Mayne, A.W., Jr., "Analysis of Laminar Boundary Layers on Right Circular Cones at Angle of Attack Including Streamline-Swallowing Effects," AEDC-TR-72-134, Oct. 1972.

[40]Mayne, A.W., Jr., "Calculation of the Boundary-Layer Flow in the Windward Symmetry Plane of a Spherically Blunted Axisymmetric Body at Angle of Attack, Including Streamline-Swallowing Effects," AEDC-TR-73-166, Oct. 1973.

[41]Cohen, C.B. and Reshotko, E., "The Compressible Laminar Boundary Layer With Heat Transfer and Arbitrary Pressure Gradient," NACA Report 1294, 1956.

[42]Walker, G.K. and Schumann, B.A., "The Growth of Turbulent Boundary Layers," General Electric Co., TIS No. R615D123, July 1961.

[43]Vaglio-Laurin, R., "Laminar Heat Transfer on Three-Dimensional Blunt Bodies in Hypersonic Flow," *ARS Journal*, Vol. 29, No. 2, Feb. 1959, pp. 123-129.

[44]Bushnell, D.M., Jones, R.A., and Huffman, J.K., "Heat-Transfer and Pressure Distributions on Spherically Blunted 25° Half-Angle Cone at Mach 8 and Angles of Attack Up to 90°," NASA TN D-4792, Oct. 1968.

[45]Cooper, M. and Mayo, E.E., "Measurements of Local Heat Transfer and Pressure on Six 2-Inch-Diameter Blunt Bodies at a Mach Number of 4.95 and at Reynolds Numbers Per Foot Up tp 81×10^6," NASA Memo, 1-3-59L, March 1959.

[46]Hall, J.R. and Speegle, K.C., "Preliminary Results From a Free-Flight Investigation of Boundary-Layer Transition and Heat Transfer on a Highly Polished 8-Inch-Diameter Hemisphere-Cylinder at Mach Number of 4.95 and at Reynolds Numbers Per Foot Up to 81×10^6," Up to 17.7×10^6," NACA RML57D18C, May 1957.

[47]Carter, H.S. and Bressette, W.E., "Heat Transfer and Pressure Distribution on Six Blunt Noses at a Mach Number of 2," NACA RML57C18, April 1957.

[48]Chavin, L.T. and Speegle, K.C., "Boundary-Layer Transition and Heat-Transfer Measurements From Flight Tests of Blunt and Sharp 50° Cones at Mach Numbers From 1.7 to 4.7," NACA RML57D04, April 1957.

[49]Van Driest, E.R., "Turbulent Boundary Layers in Compressible Fluids," *Journal of Aerospace Sciences*, Vol. 18, No. 3, March 1956, pp. 145-160, 216.

[50]Zoby, E.V. and Graves, R.A., Jr., "A Computer Program for Calculating the Perfect Gas Inviscid Flow Field About Blunt Axisymmetric Bodies at an Angle of Attack of 0°," NASA TM X-2843, Dec. 1973.

[51]Falanga, R.A. and Olstad, W.B., "An Approximate Inviscid Radiating Flow-Field Analysis for Sphere-Cone Venusian Entry Vehicles," AIAA Paper 74-758, July 1974.

[52]Zoby, E.V., Sutton, K., Olstad, W.B., and Moss, J.N., "An Approximate Inviscid Radiating Flow-Field Analysis for Outer Planet Entry Probes," *Progress in Astronautics and Aeronautics: Outer Planet Entry Heating and Thermal Protection*, Vol. 64, edited by R. Viskanta, AIAA, New York, 1979, pp. 42-64.

[53]Moss, J.N., Simmonds, A.L., and Anderson, E.C., "The Impact of Turbulence on a Radiating Shock Layer With Coupled Ablation Injection," AIAA Paper 78-1186, July 1978.